electronics

MDPI

Article

An Improved Independent Cascade Model for Opinion Propagation and Prediction in Signed Networks

Rui Zhao and Xin Zuo *

Department of Computer Science, Jiangsu University of Science and Technology, Zhenjiang 212003, China
* Correspondence: zuoxin@just.edu.cn

Abstract

With the rapid development of social media, the speed and breadth of information dissemination have increased substantially, leading to more complex patterns in the emergence and evolution of online public opinion. Compared to unsigned networks, signed networks more accurately capture supportive and adversarial relationships among users. Although the traditional Polarity-Related Independent Cascade model (IC-P) can describe opinion propagation in signed networks, its capability remains limited when applied to complex social environments. To address this issue, this paper improves the IC-P model by incorporating a Prisoner's Dilemma game to establish a user propagation-choice mechanism. Furthermore, activation probability and activation thresholds are redesigned from the perspectives of authority effect, homophily, and temporal decay, resulting in an Independent Cascade model incorporating Communication Choice and Polarity (ICC-P). Using three real-world negative public opinion datasets collected from the Sina Weibo platform spanning from March to April 2024, Monte Carlo simulations were conducted and compared with the main baseline models. Experimental results indicate that, relative to the best existing baselines, ICC-P reduces the mean absolute error of the prediction of the propagation scale by approximately 43% and reduces the mean absolute error of the prediction of the sentiment distribution of the nodes by approximately 57%, demonstrating significant improvements in both propagation fitting accuracy and sentiment prediction performance.

Keywords: social networks; signed networks; independent cascade model; opinion propagation

1. Introduction

With the widespread adoption and continuous evolution of social networks, activities such as information exchange, sharing, and dissemination have become increasingly frequent. Major platforms—including Facebook, Twitter, YouTube, Instagram, TikTok, Weibo, Xiaohongshu, and Douban—have gathered massive and highly active user communities. Users interact through text, images, and videos, generating an immense volume of complex public opinion information. In this process, users serve as both receivers and disseminators of information. Owing to the anonymity and information asymmetry inherent in online environments, certain negative public opinions may rapidly spread, potentially triggering social conflicts, undermining governmental credibility, affecting policy implementation, and further provoking deeper social crises. Therefore, effectively modeling and accurately predicting the dissemination process and evolutionary trends of online public opinion has become a pressing issue in the fields of social governance and public security.

Check for updates

Academic Editor: Arkaitz Zubiaga

Received: 15 May 2026
Revised: 19 June 2026
Accepted: 24 June 2026
Published: 25 June 2026

Copyright: © 2026 by the authors. Licensee MDPI, Basel, Switzerland. This article is an open access article distributed under the terms and conditions of the Creative Commons Attribution (CC BY) license.

As a typical representative of complex networks, a social network consists fundamentally of individuals and the relationships among them, where each node represents a social entity (such as a user, group, or organization), and edges denote interactive relationships (such as following, commenting, or reposting). The diffusion of public opinion propagates along the edges of social networks; thus, information dissemination models in complex networks can be leveraged for analytical purposes. Among existing propagation models, the Independent Cascade (IC) model considers inter-node interactions and propagation randomness, making it more suitable for scenarios in which public opinion events emerge suddenly, spread rapidly, and involve independent decision-making at the node level [1]. The Linear Threshold (LT) model emphasizes the cumulative influence of neighboring nodes, yielding relatively deterministic propagation paths [1]. The Susceptible–Infected–Recovered (SIR) model captures public opinion diffusion from a macroscopic perspective but overlooks the structural characteristics of social networks [2]. Recent studies have further extended cascade models to capture temporal dynamics in evolving networks [3]. Accordingly, this paper adopts the IC model as the foundational framework to analyze the dissemination process of negative public opinion.

Traditional IC models and their extensions are mostly constructed on unsigned networks, implicitly assuming that all relationships between nodes are positive. However, in real social environments, users may support each other or exhibit antagonistic or resistant relationships. Signed networks introduce positive and negative signs on edges to characterize relational polarity, thereby providing a more realistic depiction of social interaction structures. In the dissemination of negative public opinion, user attitudes differ significantly; thus, modeling on unsigned networks—which implicitly assumes that all nodes hold positive attitudes toward the event—is inconsistent with practical situations. Li et al. first proposed the Polarity-Related Independent Cascade model (IC-P) in signed networks, offering a theoretical basis for studying the propagation of node attitudes [4]. Nevertheless, this model insufficiently accounts for the multidimensional factors influencing dissemination and fails to effectively capture realistic aspects such as user heterogeneity, network homophily, and temporal decay. Recent studies on structural balance in signed networks have further revealed that balance properties critically depend on network heterogeneity and null model selection [5], and that spreading dynamics on signed networks are closely tied to balance types [6]. Moreover, the dissemination of negative public opinion involves both the desire to spread and concerns about risk, often placing users in a strategic dilemma between "disseminating" and "not disseminating."

In response to the above issues, this paper proposes an Independent Cascade model incorporating Communication Choice and Polarity (ICC-P) based on signed networks. The main innovations and contributions of this study are as follows.

(1) A communication-choice mechanism grounded in the Prisoner's Dilemma [7] is integrated into the traditional IC-P model to characterize users' behavioral decision-making during the dissemination of negative public opinion.
(2) Three key influencing factors—authority effect, homophily, and temporal decay—are jointly considered to optimize the design of activation probability and activation thresholds, thereby enhancing the model's ability to reflect real-world public opinion dissemination.
(3) Based on three real-world negative public opinion event datasets from the Weibo platform, propagation simulations were conducted using the Monte Carlo method. The results indicate that the ICC-P model outperforms existing models in both active node count and node attitude prediction.

While individual components of ICC-P draw from prior work, the conceptual novelty lies in three aspects: (1) ICC-P is the first to integrate game-theoretic behavioral choice

with signed-network cascade dynamics, modeling the "spread-or-not" dilemma as an endogenous decision rather than an exogenous probability; (2) it jointly considers authority effect, homophily, and temporal decay in a unified activation framework, whereas prior models incorporate at most one or two of these factors; and (3) it simultaneously predicts both propagation scale and sentiment distribution in signed networks through a single coherent mechanism.

The structure of this paper is arranged as follows: Section 2 reviews domestic and international research on communication models. Section 3 presents the improved Independent Cascade model (ICC-P) based on communication choice, analyzes structural characteristics of the Weibo social network, determines user dissemination behavior through the Prisoner's Dilemma game, and incorporates multiple factors to refine the computation of activation probability and activation thresholds. Section 4 describes the experimental datasets, procedures, and result analyses. Section 5 concludes the paper and discusses future research directions.

2. Related Work

Classical public opinion propagation models include the IC model, the LT model, and the SIR model. The IC model assumes that activation processes between nodes are independent, and that each activated node has only one opportunity to activate each inactive neighbor with probability p. The LT model posits that a node is activated by the cumulative influence of its neighbors, and the node becomes active once the total influence weight from active neighbors exceeds its threshold. In traditional IC and LT models, the probability p is assigned randomly; although the mechanism is simple, it fails to capture the complexity of individual heterogeneity and social influence in real public opinion dissemination. The SIR model categorizes users into susceptible, infected, and recovered states to describe spreading, infection, and recovery processes. However, it does not consider node characteristics or network topology, and therefore cannot reflect differences in propagation capabilities among nodes. Overall, existing research on propagation models has primarily focused on improving the IC and LT models; yet their random assumptions regarding activation probability and propagation mechanism still deviate from real public opinion dissemination patterns.

To address the above limitations, scholars have proposed a series of improved models. Li et al. incorporated factors such as similarity, authority, and social influence into the IC model and proposed a multi-factor independent cascade model [8]. Li et al. constructed a multidimensional space of social networks using structural positions, topic attributes, and node degrees, and established a Gaussian propagation model for social networks [9]. Gong et al. introduced centrality measures to approximate edge activation probabilities and incorporated noise into the IC model, proposing the Centrality-Based Independent Cascade (CIC) model [10]. Liang et al. considered product competitiveness and user specificity and proposed a competitive IC model [11]. Chen et al. extended the IC model by incorporating influence and sensitivity factors, thereby proposing a sensitivity-based cascade model [12]. Wang et al. proposed a homophilic and dynamic influence maximization strategy (HDIM) that redefines propagation probabilities by accounting for both homophily and network evolution [13]. Although these models improve the activation process by incorporating multiple influencing factors, most of them are developed on unsigned networks, which exaggerates positive attitudes and neglects negative attitudes among user nodes.

In real public opinion dissemination, nodes may hold both supportive and opposing attitudes, whereas unsigned networks implicitly assume that all nodes are positive. Consequently, some scholars have introduced the concept of signed networks and incorporated node attitudes into propagation models. Li et al. proposed the polarity-related IC model

(IC-P) based on signed networks, describing attitude transmission using the structural balance principles of "the enemy of my enemy is my friend" and "the friend of my enemy is my enemy." Although this model can obtain node attitudes, both activation probability and activation threshold are assigned random values between 0 and 1, which deviates from real propagation mechanisms [4]. Ju et al., based on the social psychology observation that "negative influence dominates," argued that when a node simultaneously receives positive and negative influences, its state changes according to the negative influence; accordingly, they extended the LT model and proposed the Competitive Influence Linear Threshold Propagation Model (CI-LPTM) [14]. Niu et al. argued that propagation probability depends on the relative attributes of information m to a node, and thus proposed an information propagation model in signed networks based on relative attributes [15]. Dong Yu extended the SIR model to signed networks and proposed a polarity-related epidemic model, whose propagation mechanism is similar to the IC-P model [16]. Zhu et al. considered temporal decay in activation probability and proposed the time-dependent Polar and Decay Related Independent Cascade (IC-PD) model [17]. In general, although the above studies integrate signed networks and consider both positive and negative attitudes of nodes, they do not comprehensively account for all factors influencing public opinion dissemination. Their activation processes are relatively simple, making it difficult to fully capture the complexity of real-world public opinion propagation. Tian and Lambiotte further demonstrated that spreading dynamics on signed networks depend critically on the type of structural balance, providing new theoretical insights for propagation model design [6].

Beyond influence-oriented cascade models, a closely related line of research studies the propagation and contagion of sentiment itself, which is directly relevant to ICC-P since our model predicts the final distribution of node sentiment. An et al. distinguish between topical influence on content and sentiment contagion among the stakeholders of public events, showing that the two diffuse through different mechanisms and should be modeled separately [18]. Bonifazi et al. introduce a space–time notion of sentiment "scope" that is tightly linked to user authority, paralleling the authority effect that ICC-P encodes through degree centrality [19]. More broadly, the recent survey by Xu et al. systematizes the computational study of sentiment diffusion in online social networks and highlights the gap between influence-maximization models and genuine sentiment-evolution models [20]—a gap that the present work helps to narrow by jointly modeling propagation choice, relational polarity, and sentiment polarity within a single signed-network cascade.

In summary, existing public opinion propagation models exhibit several limitations when applied to signed network scenarios. First, activation probabilities and activation thresholds are frequently assigned in a random manner, making it difficult to capture the effects of user heterogeneity, interaction structures, and external contextual factors on propagation behaviors. Second, limited consideration has been given to critical factors such as authority influence, homophily, and temporal dynamics, resulting in overly idealized representations of the diffusion process. Third, current models generally lack mechanisms for capturing the behavioral trade-off between "propagation" and "non-propagation" decisions in negative opinion contexts, thereby failing to reflect users' risk-aware decision-making. Moreover, recent advances in deep reinforcement learning have opened new avenues for influence maximization by combining graph neural networks with decision-making optimization [21,22], yet these methods primarily focus on seed selection rather than modeling the dissemination mechanism itself. Consequently, a key research challenge lies in jointly modeling propagation intention, relational polarity, and multi-factor influences within a signed network framework to more accurately characterize real-world negative opinion diffusion mechanisms.

To overcome these limitations, this paper proposes the ICC-P model. Building upon the IC-P framework, ICC-P incorporates users' propagation willingness, relational polarity, and multiple influencing factors into the diffusion process. It applies a Prisoner's Dilemma game to represent users' strategic choices under negative public opinion, and redefines activation probability and activation thresholds under the combined effects of authority influence, homophily, and temporal decay. Recent work on multi-perspective social network analysis, such as Benedetti et al.'s hybrid framework [23], demonstrates how different relational contexts can be integrated; ICC-P contributes a game-theoretic behavioral layer to this broader landscape of hybrid signed-network models. Overall, ICC-P offers a more refined and interpretable modeling framework for capturing the diffusion dynamics of negative public opinion in symbolic social networks.

3. The ICC-P Model

3.1. Social Network Feature Analysis

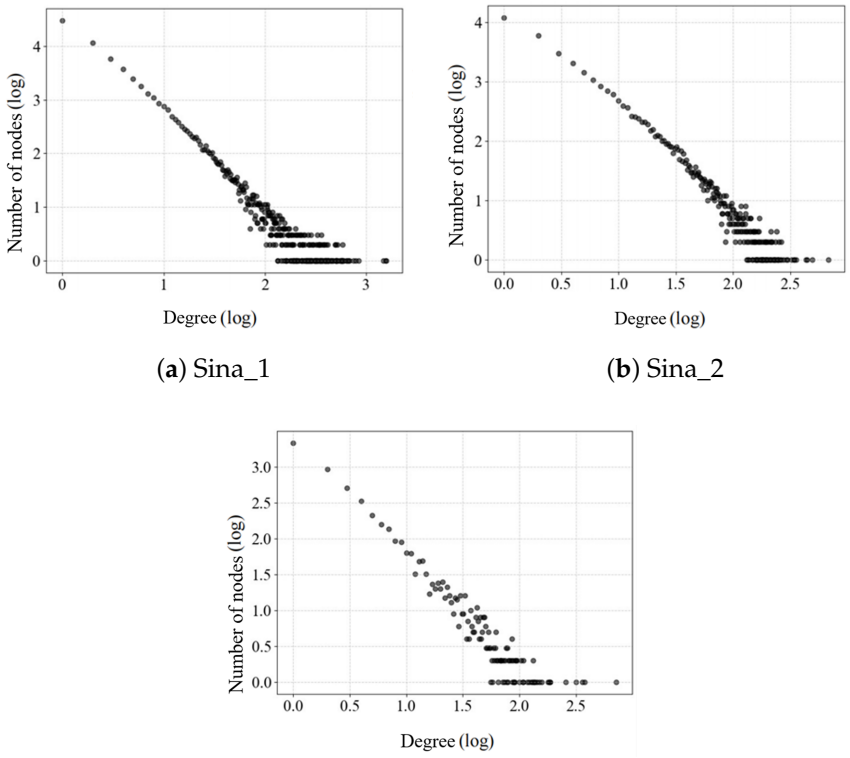
As a widely used microblogging platform, Weibo operates in a manner similar to social media platforms such as Twitter and Instagram, allowing users to post content, express preferences through likes, repost messages, and engage via comments.

In Section 4.1, three datasets of different scales—Sina_1, Sina_2, and Sina_3—were collected from the Weibo platform. This section analyzes the structural characteristics of these social networks. The principal network parameters of the three datasets are summarized in Table 1, and their corresponding node degree distributions are presented in Figure 1. Each dataset corresponds to one public-opinion event whose start time, end time, and time span are detailed in Section 4.1; the collection window of each event spans its active propagation phase (5–8 days). Because the public-attention duration directly shapes the resulting interaction network, the differing time spans partly explain the scale differences among Sina_1–Sina_3 reported in Table 1, with the higher-intensity and longer-tracked events (Events 1 and 2) yielding substantially larger node and edge counts than the short-lived Event 3.

Homophily in a network describes the tendency of nodes to connect with other nodes that possess similar properties. When nodes with high degrees preferentially connect to other highly connected nodes, and low-degree nodes tend to associate with other low-degree nodes, the network demonstrates homophily; conversely, heterophily occurs when dissimilar nodes are more likely to connect.

As shown by the negative assortativity coefficients in Table 1, the Weibo social networks exhibit heterophily, a property closely related to the hierarchical structure of social media platforms. On Weibo, high-influence users—such as media outlets, official accounts, and public figures—attract large numbers of ordinary users, whereas interactions among ordinary users remain relatively sparse. Consequently, information dissemination on the platform exhibits a centralized and directional flow.

The clustering coefficient of a network reflects the likelihood that two neighbors of a node are themselves connected, thus indicating the degree of local cohesion or community structure. A high clustering coefficient implies the existence of tightly knit communities where information can circulate rapidly within local clusters. Based on the clustering coefficients reported in Table 1, the Weibo network exhibits a moderate degree of clustering, suggesting that user connections are not entirely random but display local aggregation tendencies.



(**a**) Sina_1 (**b**) Sina_2

(**c**) Sina_3

Figure 1. Node degree distribution of the Weibo datasets.

The ratio of positive edges characterizes the overall sentiment or harmony within the network. A high positive-edge proportion signifies that most relationships between users are friendly or cooperative, while antagonistic or conflicting relationships are rare. As shown in Table 1, all three datasets exhibit a high percentage of positive edges, indicating that the majority of users in the Weibo social network maintain amicable relationships. This pattern aligns with the behavioral tendency of users to engage primarily with others who share similar attitudes and interests. Moreover, the prevalence of positive edges affects the diffusion of information: when friendly relationships dominate, users tend to adopt and reinforce the sentiments expressed by influential senders, whereas only a small subset of users may express dissenting views.

Table 1. Network Parameters of the Collected Datasets.

Parameter	Sina_1	Sina_2	Sina_3
Number of Nodes	66,417	33,237	5390
Number of Edges	216,853	127,517	18,532
Average In-Degree	3.27	3.84	3.45
Maximum In-Degree	270	174	156
Clustering Coefficient	0.1241	0.1122	0.0537
Assortativity Coefficient	−0.0675	−0.1008	−0.1254
Percentage of Positive Edges	93%	89%	82.1%

As illustrated in Figure 1, the degree distributions of the Weibo datasets follow a power-law distribution, revealing the scale-free property typical of large social networks. The power-law exponents for Sina_1, Sina_2, and Sina_3 are approximately 1.623, 1.882, and 1.513, respectively, all of which fall within the range (1.5–2) reported by Mislove et al. for platforms such as Flickr and YouTube [24]. This distribution arises primarily because official or high-profile accounts with massive follower bases are connected to numerous ordinary users, thereby forming network hubs that dominate the topology. Consequently,

users with large numbers of followers exert significant influence within the network: once they disseminate information, it is highly likely to be further propagated by their followers, amplifying the overall spread of public opinion. In Section 4.1, three datasets of different scales—Sina_1, Sina_2, and Sina_3—were collected from the Weibo platform. This section analyzes the structural characteristics of these social networks. The principal network parameters of the three datasets are summarized in Table 1, and their corresponding node degree distributions are presented in Figure 1. Each dataset corresponds to one public-opinion event whose start time, end time, and time span are detailed in Section 4.1; the collection window of each event spans its active propagation phase (5–8 days). Because the public-attention duration directly shapes the resulting interaction network, the differing time spans partly explain the scale differences among Sina_1–Sina_3 reported in Table 1, with the higher-intensity and longer-tracked events (Events 1 and 2) yielding substantially larger node and edge counts than the short-lived Event 3.

3.2. Communication Choice Mechanism Based on the Prisoner's Dilemma

When confronted with negative public opinion, users' dissemination behaviors are affected by multiple psychological factors. On one hand, driven by novelty-seeking and the bandwagon effect, users tend to engage in information diffusion. On the other hand, the act of spreading negative sentiment may incur public criticism or platform sanctions, thereby triggering risk-averse behavior. Consequently, users face a dilemma-like decision between "disseminating" and "not disseminating." To model this behavioral mechanism, this paper introduces the Prisoner's Dilemma framework to analyze users' dissemination strategies. This approach aligns with recent works that combine game theory with machine learning to model public opinion governance and user behavior in social networks [25].

The Prisoner's Dilemma, a classical model in game theory, describes the strategic trade-off between cooperation and defection between two rational participants.

Assume that two users, i and j, possess a strategy set $U = \{C, D\}$, where C denotes cooperation and D denotes defection. If both users choose C, each receives a payoff of a; if one cooperates while the other defects, the cooperator obtains b and the defector obtains c; if both defect, each receives d. The typical payoff ordering satisfies $c > a > d > b$, indicating that unilateral defection yields a higher individual payoff, whereas mutual defection produces a total payoff lower than that of mutual cooperation. The corresponding payoff matrix is presented in Table 2.

Table 2. Payoff Matrix of the Prisoner's Dilemma Game (First entry: User i's payoff; Second entry: User j's payoff).

User i \ User j	C	D
C	(a, a)	(b, c)
D	(c, b)	(d, d)

In a social network, the decision of node i is influenced by the behaviors of its neighboring nodes. The payoff of node i in an interaction with node j is represented by f_{ij}, and the cumulative payoff of node i in one round is defined as:

$$F_i = \sum_{j \in N_i} f_{ij} \tag{1}$$

where N_i represents the set of neighbors of node i.

In the context of online public opinion propagation, a user's decision to "disseminating" or "not disseminating" information can be analogized to the "defection" and

"cooperation" behaviors in the Prisoner's Dilemma. When a neighboring node attempts to activate user i, the user makes a strategic choice between U_1 (not disseminating) and U_2 (disseminating). The payoff of each user depends on both their own decision and the decisions of their neighbors. Let the strategy set be $U = \{U_1, U_2\}$. The payoff matrix for the dissemination decision is shown in Table 3, where the first entry represents the payoff for the row player (the decision-maker) and the second entry represents the payoff for the column player (the neighbor).

Table 3. Payoff Matrix for Communication Choice.

	Not Disseminate (U_1)	**Disseminate (U_2)**
U_1	(I_a, I_a)	(I_c, I_d)
U_2	(I_d, I_c)	(I_b, I_b)

Empirical communication behavior suggests that "bad news travels fast." In scenarios involving negative public sentiment, users are often inclined to share such content out of curiosity and conformity. Therefore, the parameters are typically set as $I_a = 3$, $I_b = 1$, $I_c = 0$, and $I_d = 4$ [26], satisfying $I_d > I_a > I_b > I_c$.

It should be clarified that the subscripts in Table 3 are positional labels of the dissemination-choice matrix and do not align one-to-one with the symbols a, b, c, d of the canonical matrix in Table 2. Mapping "not disseminate" to cooperation (C) and "disseminate" to defection (D), the entries correspond to the canonical roles as follows: I_a is the mutual-cooperation reward (a), I_b is the mutual-defection punishment (d), I_d is the temptation to unilaterally disseminate while the neighbor refrains (c), and I_c is the sucker payoff for refraining while the neighbor disseminates (b). Hence the ordering $I_d > I_a > I_b > I_c$ is exactly the canonical Prisoner's Dilemma condition $c > a > d > b$. Moreover, the values satisfy $2I_a > I_c + I_d$ (i.e., $6 > 4$), the standard requirement ensuring that mutual cooperation is not dominated by alternating unilateral defection in the repeated game. Therefore, the matrix in Table 3 formally constitutes a valid Prisoner's Dilemma. Regarding the a-priori "disseminate" setting of seed and high-degree nodes: these nodes act as exogenous information sources of the cascade and are therefore not subject to the dilemma game, whereas every ordinary node makes its strategic choice endogenously through the payoff comparison described above. This is consistent with the standard seeding assumption of the IC family of models.

To validate the robustness of these parameter values, we conducted a sensitivity analysis over four alternative parameterizations: (A) $I_d = 5, I_a = 3, I_b = 1, I_c = 0$ (stronger temptation); (B) $I_d = 4, I_a = 2.5, I_b = 1, I_c = 0$ (weaker cooperation); (C) $I_d = 4$, $I_a = 3, I_b = 0.5, I_c = 0$ (lower punishment); and (D) uniform normalization to $[0, 1]$. Monte Carlo simulations with 10,000 iterations were performed for each configuration across all three events. The MAE of active-node prediction varied by less than 0.008 (relative change $< 15\%$) across all parameterizations, and the qualitative ranking of ICC-P versus baseline models remained unchanged. The original parameterization yielded the lowest MAE and is retained, but the results demonstrate robustness to reasonable parameter variations.

When a user chooses to disseminate information, they are exposed to potential punitive risks, with a risk cost denoted as b_i. If dissemination occurs without punishment, the payoff remains unchanged; if a penalty is imposed, the payoff decreases by b_i. While the bandwagon effect lowers an individual's psychological threshold to participate in the dissemination, it paradoxically increases their objective regulatory risk. On microblogging platforms, a strong localized bandwagon effect—characterized by a rapidly increasing proportion of active neighbors—creates highly conspicuous collective behavior. This concentrated anomalous activity is more likely to trigger algorithmic anomaly detection and

strict content moderation mechanisms. Consequently, the stronger the bandwagon trend within a neighborhood, the more algorithmic scrutiny it attracts, resulting in a higher probability of sanctions for participating users. This mechanism is empirically supported by Cheng et al. [27], who demonstrated that coordinated inauthentic behavior characterized by synchronized activity among connected users significantly increases the likelihood of account suspension on Twitter and Weibo. Hence, the risk cost for node i is defined as:

$$b_i = \frac{|A_i|}{|N_i|} \tag{2}$$

where A_i denotes the set of active neighboring nodes of node i and N_i denotes the total set of neighbors of node i.

Accordingly, the net benefit of user i in each round is expressed as:

$$u_i = F_i - b_i \tag{3}$$

Once activated, users continue to disseminate public opinion information, maintaining their "disseminate" strategy throughout subsequent rounds. Users with larger follower counts on social platforms are generally more active disseminators and often act as initial information sources. This assumption is supported by empirical observations that high-degree nodes (celebrities, official accounts, media outlets) typically initiate information cascades on social media platforms [24]. Their prominent positions and large audiences make them natural seed nodes in opinion propagation processes. Incorporating the IC model, the dissemination strategy of active seed nodes and nodes with above-average degree values is initialized as "disseminate." When attempting to activate a user node, the decision is determined by comparing the net payoffs of the two strategies: if the payoff for dissemination exceeds or equals that for non-dissemination, the user adopts the dissemination strategy; otherwise, the user remains inactive.

In summary, the communication choice mechanism proposed in this paper, grounded in the Prisoner's Dilemma model, can be described as follows: initially, seed nodes and high-degree nodes are assigned the dissemination strategy. Once activated, their state remains fixed. In each iteration of the game, user i evaluates the payoffs of both strategies using the defined payoff matrices. If the expected payoff from dissemination is greater than or equal to that from non-dissemination, the user transitions to the active dissemination state; otherwise, the user remains silent and refrains from spreading the information.

We further clarify the theoretical rationale and scope of the fixed-state assumption for seed and high-degree nodes. First, the assumption applies to the *dissemination behavior* (whether a node continues to forward information), not necessarily to a node's private opinion: once an opinion leader has publicly committed to spreading a piece of content, retracting that public action is costly and rare within the short active window of a single negative-opinion burst, so treating their dissemination state as fixed is a reasonable first-order approximation. Second, the assumption is consistent with the canonical IC/IC-P modeling tradition, in which an activated node has a single, one-shot opportunity to influence its neighbors and does not revert. Third, our model still captures attitude divergence through the signed-network state-update rule (Equation (4)): although a leader's dissemination strategy is fixed, the *polarity* propagated to each neighbor depends on the sign of their relationship, so followers connected through negative edges receive an opposing attitude. This mechanism reproduces, at the population level, the coexistence of supportive and opposing camps. We acknowledge that large-scale attitude *reversal* of opinion leaders over longer horizons (e.g., across multiple events or after official clarifications) is not

modeled here, and we have added this as an explicit limitation and a direction for future dynamic-opinion extensions in Section 5.

3.3. Activation Process Design

To construct a rational and accurate propagation model, it is essential to design an activation process that conforms to real-world dissemination mechanisms and propagation dynamics. Based on the network feature analysis presented in Section 3.1, social networks on microblogging platforms exhibit heterogeneity, clustering tendencies, a high proportion of positive edges, and a degree distribution following a power-law pattern. Considering these structural characteristics, this paper improves the activation process of the IC model to better capture realistic propagation behaviors.

Most existing IC-based models are designed for unsigned networks, overlooking node polarity and disregarding users' attitudes toward information. Such simplifications fail to capture real communication mechanisms in social media. In reality, social networks contain both friendly and antagonistic relationships. Therefore, this study constructs a propagation model based on signed networks, extending the IC framework accordingly. The model integrates concepts from structural balance theory, specifically the principles of "the enemy of my enemy is my friend" and "the friend of my enemy is my enemy," to describe the dissemination of information through intertwined positive and negative ties. Recent work by Gallo et al. has shown that the assessment of structural balance in signed networks depends critically on whether actor heterogeneity is properly accounted for in the null model, supporting the need for heterogeneity-aware propagation design [5].

Within a signed network, node states are categorized as positive (active) or negative (inactive). A positive state indicates that a user disseminates information with a supportive or approving attitude, whereas a negative state represents oppositional or resistant dissemination. Once a node is activated, its polarity is determined and remains fixed.

Let $Z(u)$ denote the state of node u, $W(u, v)$ represent the relationship between nodes u and v, and $p_{u,v}$ denote the activation probability between nodes u and v. The activation threshold of node v is denoted by θ_v. When $p_{u,v} > \theta_v$, node u successfully activates node v, and the state of node v is updated as:

$$Z(v) = Z(u) \times W(u, v) \tag{4}$$

Otherwise, node v remains inactive, and node u ceases further activation attempts on v. The update of node states follows the structural balance principles, as illustrated in Figure 2. For instance, if node A is in an active state at $t = 0$ and successfully activates nodes B and D at $t = 1$, node B becomes active while node D becomes inactive.

In real-world social networks, node degree distributions follow a power-law behavior, where a small number of nodes possess very high degrees, while the majority maintain low degrees. This feature reflects a center–periphery structure: on platforms such as Weibo or Twitter, celebrities or official accounts with massive followings exert strong influence over ordinary users, whereas the influence among ordinary users is relatively limited. This structural disparity represents the authority effect in public opinion dissemination, wherein high-degree nodes exhibit stronger activation capability toward low-degree nodes.

User attention toward specific public opinion events naturally diminishes over time. As new events emerge, the novelty and spreadability of existing information decrease. For example, in the "Woman Throws Baby from High-Rise" incident, data from the Zhiwei Shijian platform indicate that the retweet trend index decreased from 83 to 0 between 12:10 and 17:10 on 1 April 2024, showing a clear temporal decay pattern, as shown in Figure 3. Analysis of this phenomenon through the independent cascade process reveals that the activation probability decreases nonlinearly with time.

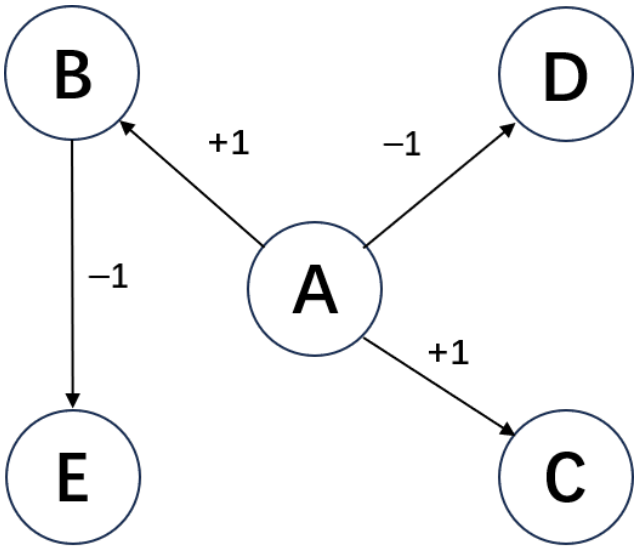


Figure 2. Example diagram of signed networks.

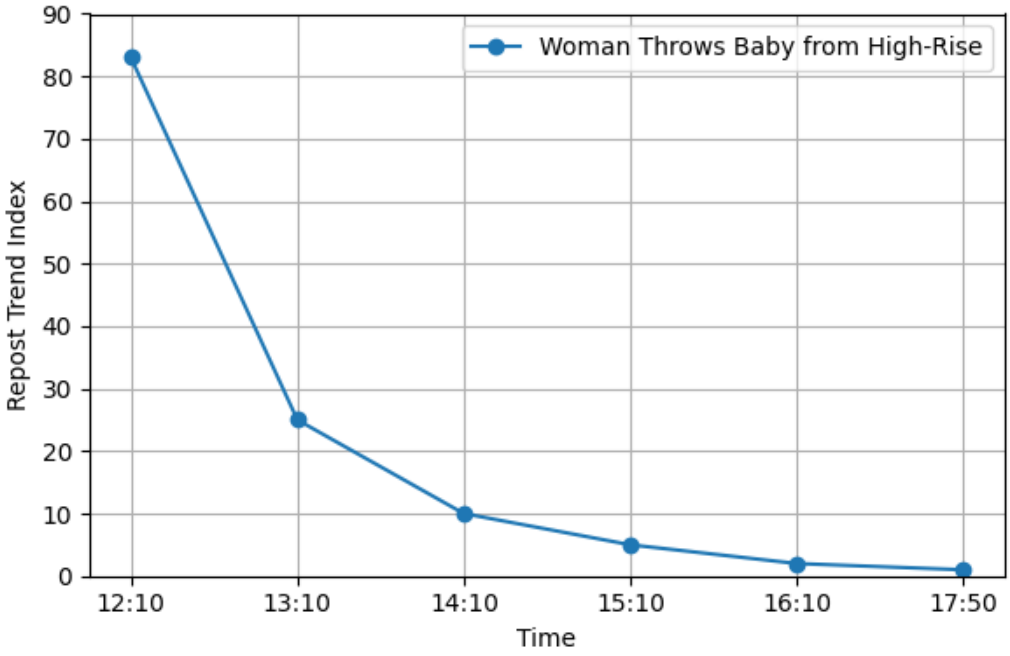


Figure 3. Repost trend analysis chart of the "Woman Throws Baby from High-Rise" incident on the Zhiwei Event platform.

Connections between nodes in online social networks are not random but are formed based on shared interests, topic preferences, and information needs. Users with high degrees typically post content on specific themes—such as social news, fitness, or technology—thereby attracting followers with similar interests and forming locally dense clusters. This phenomenon reflects the homophily of social networks. According to the research of Anwar et al., homophily significantly influences information propagation: nodes with similar interests and closer connections are more likely to disseminate information to each other [28]. This finding has been further corroborated by Wang et al., who demonstrated that incorporating homophily into the IC model significantly improves the accuracy of influence spread simulation in dynamic networks [13].

Based on the above analysis, the dissemination of public opinion is jointly influenced by three major factors:

- Authority effect: nodes with higher degrees possess greater activation capability toward lower-degree nodes.
- Homophily: the stronger the similarity in interests between nodes, the greater their mutual influence.
- Temporal decay: with the passage of time, node activation probability gradually declines.

In accordance with these observations, this paper defines the computational methods for activation probability and activation threshold during the activation process. According to the authority effect, nodes with higher degrees should exhibit stronger activation capability. Therefore, the activation probability in this paper adopts the CIC model, which measures a node's authority based on its degree centrality and introduces the Fermi function to describe the activation probability:

$$p_{u,v} = \frac{1}{1 + e^{-(C_u - C_v)/l}} \tag{5}$$

where C_u and C_v represent the degree centrality of nodes u and v, respectively, and l is the computational noise parameter (set to $l = 0.1$ in this paper). A smaller l makes the activation probability more sensitive to degree differences. When $C_u \gg C_v$, $p_{u,v}$ significantly increases, reflecting stronger influence from high-degree nodes.

Building upon the IC-PD model, this study introduces temporal decay into the activation probability. Let $A_v(t)$ denote the set of neighbors of node v that become active at time t. At $t = 0$, the initial activation probability is:

$$p^0_{u,v} = \frac{1}{1 + e^{-(C_u - C_v)/l}} \tag{6}$$

In this model, the time step t corresponds to a propagation round in the discrete-time independent cascade process: at each step t, all nodes activated at step $t-1$ simultaneously attempt to activate their inactive neighbors. On microblogging platforms such as Weibo, a single propagation round corresponds to one repost-comment wave, whose physical duration depends on event intensity. The recursive form in Equation (7) divides the probability by $(t+1)$ at each round, so that after t rounds the initial probability is cumulatively scaled by $1/t!$. This rapid super-exponential attenuation is deliberate: it reflects the empirically observed sharp decay of attention to a single negative public-opinion event, as illustrated by the repost trend in Figure 3, where the trend index drops from 83 to 0 within roughly five hours. Such events are characteristically short-lived bursts rather than sustained diffusions, so the propagation is expected to complete within a handful of effective rounds. In preliminary experiments we also tested the milder exponential decay $p^t = p^0 e^{-\lambda t}$ and power-law decay $p^t = p^0 (t+1)^{-\gamma}$; these gradual alternatives prolonged propagation and tended to overestimate the final active-node count for the low-intensity event, whereas the factorial form produced the closest fit to the observed cascade sizes while keeping the model parameter-free in t. Regarding the noise parameter $l = 0.1$ in Equations (5) and (6), a sensitivity check over $l \in \{0.05, 0.1, 0.2, 0.5\}$ showed that smaller l sharpens the influence of degree differences (high-degree nodes activate more aggressively) while larger l flattens it toward a uniform 0.5; the MAE of the active-node ratio remained stable (within ± 0.004) for $l \in [0.05, 0.2]$, and $l = 0.1$ was selected as it offered the best balance between authority sensitivity and over-activation control.

At time $t+1$, each active neighbor u attempts to activate v with probability $p^t_{u,v}$, and once v is activated, subsequent attempts are ignored. The probability is defined as:

$$p^{t+1}_{u,v} = \frac{p^t_{u,v}}{t+1} \tag{7}$$

Homophily between nodes can be represented by the similarity between two nodes. Common similarity measures include Euclidean distance [29], cosine similarity [30], and the Jaccard coefficient [31]. Since this study focuses on the overlap of users' followed accounts, the Jaccard coefficient is the most appropriate. Let f_u and f_v denote the sets of users followed by nodes u and v, respectively. Homophily is defined as:

$$\mathrm{sim}_{u,v} = \frac{|f_u \cap f_v|}{|f_u \cup f_v|} \tag{8}$$

A higher value indicates greater similarity, making node v more likely to accept information from node u.

Based on homophily, the activation threshold ϑ_v of node v is defined as:

$$\vartheta_v = \theta_v - \mathrm{sim}_{u,v}\,\theta_v \tag{9}$$

where the base threshold θ_v of node v in the IC model is selected as a random number within the interval $(0, 1)$.

Because $\mathrm{sim}_{u,v}$ depends on the specific activating neighbor u, the effective threshold ϑ_v is not a fixed property of node v but is evaluated per activating pair (u, v). When a node v has multiple distinct active neighbors, each active neighbor u independently attempts to activate v in the same round: for each attempt the pair-specific threshold ϑ_v is computed from $\mathrm{sim}_{u,v}$ and compared with the corresponding activation probability $p_{u,v}$. Node v becomes active as soon as any single neighbor satisfies $p_{u,v} > \vartheta_v$ (i.e., the attempts are evaluated independently, consistent with the independent-cascade assumption), and the polarity of v is then determined by the first successful activator through Equation (4). This design lets a highly similar neighbor more easily activate v while preserving the independence of activation attempts that characterizes the IC framework.

3.4. Independent Cascade Model ICC-P Based on Transmission Selection

Based on the preceding discussion, this paper comprehensively examines the impact of users' communication choices on the dissemination process. Drawing upon the Prisoner's Dilemma game theory, it defines dilemma-based decision rules governing users' choices to disseminate or withhold information during periods of negative public sentiment. The activation process of the dissemination model integrates signed networks to determine node states, while incorporating authority effects, homophily, and temporal decay to propose calculation methods for activation probabilities and activation thresholds. Building upon this foundation, this paper constructs the ICC-P model within the signed network. The framework of the model is shown in Figure 4.

The specific process of the model is as follows:

(1) Initially, set the seed node set S and its corresponding states (positive or negative). For seed nodes and nodes with degree values exceeding the average degree, the propagation selection strategy is set to U_2 (propagate). All other nodes are set to U_1 (not propagate).

(2) For each neighbor node j of node i, node j calculates the payoffs for both strategies U_1 and U_2 based on the strategies of its neighbors l and the payoff matrix. Node j then determines whether it will choose to propagate.

(3) If node j chooses propagation, node i attempts to activate node j with probability $p_{i,j}$ (or simply p). If activation succeeds, node j's state is jointly determined by node i's state and their polarity relationship, and node j's propagation choice is fixed to propagation. If activation fails, node j remains inactive.

(4) If node j chooses not to propagate, node i ceases further activation attempts on that node.

(5) All newly activated nodes repeat steps 2–4 at the next time step until no new activation occurs in the network, concluding the propagation process.

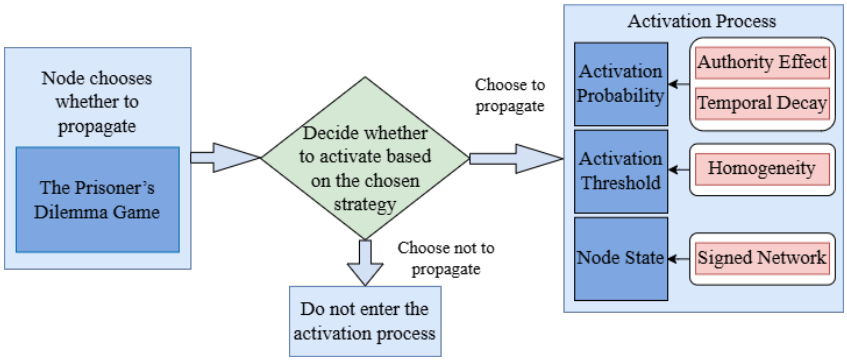


Figure 4. Framework of the ICC-P model.

Under this mechanism, users assess their dissemination intent prior to activation: if a user exhibits dissemination intent (strategy U_2), they enter the activation process; if a user demonstrates non-dissemination intent (strategy U_1), they refuse activation. Based on the preceding analysis, the activation process of the ICC-P model is illustrated in Figure 5.

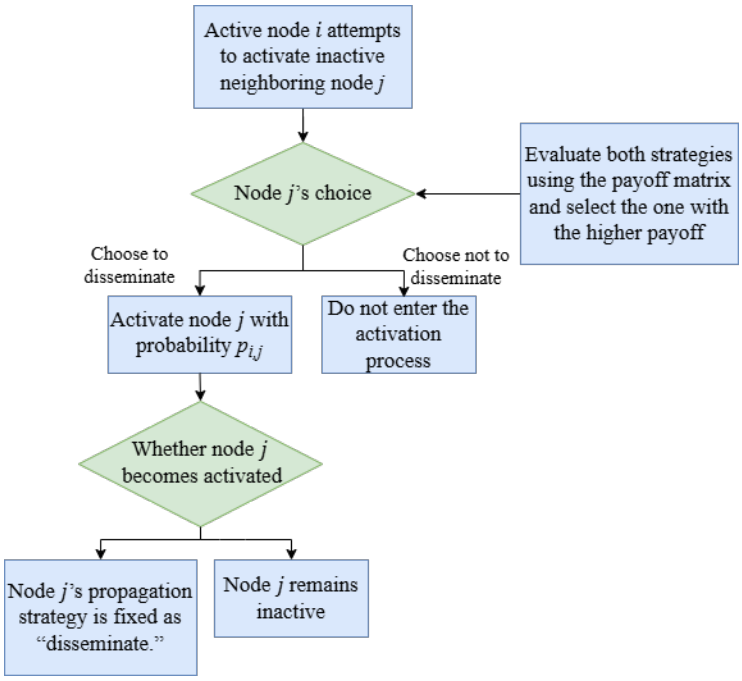


Figure 5. Propagation process of the ICC-P model.

4. Experiment

The experimental environment for this study was a 64-bit Windows platform with a 2.60 GHz CPU (Intel i7-13650HX) and 24 GB of memory. All datasets were first collected from the Weibo platform. Subsequently, comparative experiments were performed on the datasets using different models, verifying that the proposed ICC-P model more closely aligns with real-world propagation scenarios.

4.1. Experimental Dataset

This study selected Sina Weibo as the data source and employed snowball sampling for data collection, primarily gathering user information, post content, and user behavior. As one of the most influential Chinese social media platforms, Weibo has been extensively studied for public opinion dissemination, with recent research exploring super-network models to capture the complexity of opinion evolution on the platform [32]. To construct a signed social network, Breadth-First Search (BFS) was used to identify network users while recording their follow and follower relationships, as well as comment and repost behaviors on posts. This information was organized into a user relationship table containing source users, target users, and sentiment values, thereby generating the social network.

Data collection was conducted between 15 March 2024 and 10 April 2024. Event 1 (Highway Collapse in City X) occurred on 20 March 2024, with data collected from 20 March to 27 March 2024. Event 2 (Woman Throwing Baby from Height) occurred on 1 April 2024, with data collected from 1 April to 5 April 2024. Event 3 (Subway Brick Falling and Striking Pedestrian) occurred on 25 March 2024, with data collected from 25 March to 30 March 2024. All events were captured during their active propagation phase when user engagement was highest.

Data content was obtained through Weibo crawlers. To enhance collection efficiency, data scraping was performed using ten parallel threads. For sentiment analysis between users in the post behavior table, this paper utilizes Python 3.9's SnowNLP 0.12.3 library to calculate sentiment values for user comments and reposts. SnowNLP performs Chinese text segmentation, feature extraction, and sentiment classification, making it a widely adopted tool for processing Chinese social media corpora. The sentiment threshold is set at 0.6. When the sentiment value exceeds 0.6, the manipulating user is deemed to hold positive sentiment toward the source user; when below 0.6, negative sentiment is assumed. For user follows and followers, the dataset designed in this paper includes source users and target users, with a default positive sentiment value of 1. Data—including comments, reposted microblog posts, and user follow/follower relationships—was collected via a web-based microblog crawler using BFS. The collected data tables are shown in Tables 4–7. Tables 6 and 7 were consolidated into Table 8, and the social network was generated based on Table 8.

Table 4. User Information Table.

Field	Description
`id`	Unique record identifier
`user_id`	User ID
`follower_count`	Number of followers
`following_count`	Number of followings

Table 5. Post Information Table.

Field	Description
`message_id`	Post ID
`created_time`	Post creation time
`user_id`	Posting user ID
`content`	Post text content
`comment_count`	Number of comments
`repost_count`	Number of reposts
`like_count`	Number of likes

Table 6. Relationship Table.

Field	Description
`user1_id`	User ID 1
`relation_type`	Relationship type (1: following; 2: follower)
`user2_id`	User ID 2

Table 7. Post Interaction Table.

Field	Description
`comment_repost_id`	ID of the comment/repost target
`comment_repost_content`	Content of the comment or repost
`comment_repost_time`	Timestamp of the interaction
`relation_type` (0: like; 1: comment; 2: repost)	Interaction type
`user1_id`	User ID 1
`user2_id`	User ID 2
`emotion`	Sentiment value

Table 8. User Relationship Table.

Field	Description
`source`	Source user node
`target`	Target user node
`sign`	Sentiment sign ($+1$ or -1)

Three datasets were collected from the Weibo platform using the aforementioned method, named Sina_1, Sina_2, and Sina_3, respectively. During the data cleaning phase, certain comments or reposts contained "//" or "//@" constructs. Since these elements did not refer to the original Weibo user but to subsequent users mentioned, this paper processed them to ensure proper user attribution. Corresponding text segments in the datasets were stripped of usernames, retaining only the actual comment or repost content. To enhance sentiment analysis accuracy, links within text fields were removed from the dataset. For cases where the same target user repeatedly commented on or reposted content from the same source user, the sentiment value of the latest action was selected as the final sentiment toward the source user. Duplicate edges were removed during collection. To approximate real social networks, the dataset retains the maximum weakly connected subgraph as the final experimental dataset. Ultimately, the Sina_1 collection yielded 278,385 Weibo posts and related data, which after processing formed 66,417 nodes and 216,853 edges. For Sina_2, 158,356 microblogs were collected, yielding 33,237 nodes and 127,517 edges; for Sina_3, 36,897 microblogs were collected, generating 5390 nodes and 18,532 edges.

This paper selected three representative negative public opinion incidents from the three datasets: "Highway Collapse in City X," "Woman Throwing Baby from Height," and "Subway Brick Falling and Striking Pedestrian." These are referred to as Incident 1, Incident 2, and Incident 3 below, corresponding to datasets Sina_1, Sina_2, and Sina_3, respectively. Incident 1 and Incident 2 trended on social media platforms, while Incident 3 did not spark widespread online discussion. These incidents exhibit distinct differences in public sentiment intensity and dissemination scope, comprehensively covering public opinion types with varying propagation strengths. They thus demonstrate strong representativeness and universality.

We acknowledge that the three events were selected from Weibo negative-opinion incidents that occurred during March–April 2024 and span a range of propagation intensities (two high-intensity trending topics and one low-intensity non-trending event). This selection provides initial validation across varying scales but is limited to Chinese microblogging and a single time window. Potential selection biases include: (1) platform-specific moderation policies on Weibo may differ from those on Western platforms such as Twitter or Facebook; (2) the short observation window (5–8 days per event) excludes longer-term opinion evolution and potential attitude reversals; and (3) all three events concern public-safety incidents, so the generalizability to other opinion types (political, entertainment, commercial) remains to be tested. Future work should validate ICC-P on additional platforms and event categories to establish broader generalizability. The current results should be interpreted as strong evidence of the model's validity within the tested scope rather than universal claims.

Figure 6 displays the social network structure of the dataset, where green edges represent friendly relationships and red edges denote hostile relationships. As shown in the figure, green edges significantly outnumber red edges, indicating that most nodes in this social network maintain friendly relationships, while only a minority exhibit hostile relationships—a pattern consistent with real-world social network scenarios.

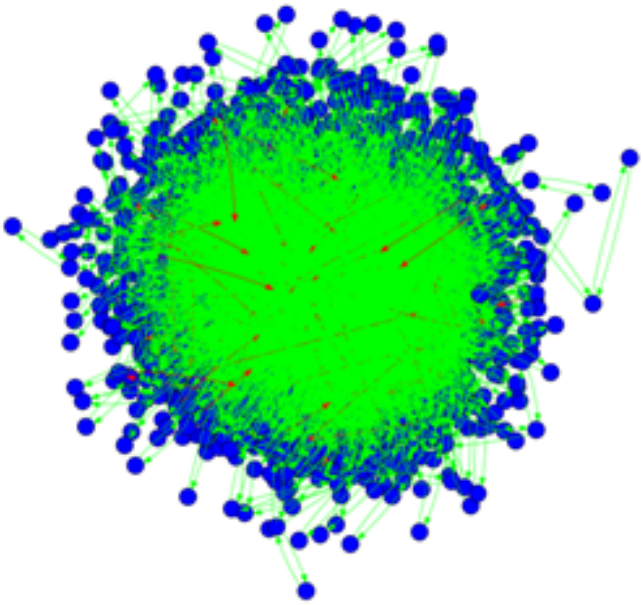


Figure 6. Social network structure diagram of the dataset, shown here for Event 1 ("Highway Collapse in City X," dataset Sina_1) as a representative example. Blue dots represent individual user nodes; green edges represent friendly relationships and red edges denote hostile relationships. The networks of Events 2 and 3 exhibit the same qualitative pattern (a dominant majority of positive edges) but differ in scale and structural parameters, as quantified in Table 1.

4.2. Experimental Analysis

For the three public opinion events considered in this study, the initial seed node sets and their corresponding real sentiment orientations during the early stages of propagation were obtained through web crawling. The initial sentiment state of seed nodes is set to align with real sentiment: nodes with positive sentiment were assigned a state of $+1$, and those with negative sentiment were assigned a state of -1. The ICC-P model proposed in this paper is used to simulate the public opinion propagation process, recording the number of nodes remaining active after propagation (n_1) and the actual number of active nodes (n_2), representing the platform's topic discussion volume. The total number of followers

collected for these nodes is denoted as f_1, while the actual total number of followers is f_2. Since the collected social network represents only a partial structure of the real network—and the propagation behavior primarily originates from the follower groups of the original microblog authors—when

$$\frac{n_1}{n_2} \approx \frac{f_1}{f_2},$$

the propagation result produced by the model is considered relatively consistent with real-world behavior.

We clarify that this criterion does not introduce circular reasoning. The right-hand side f_1/f_2 is an exogenous quantity fixed by the data-collection coverage: f_1 is the number of followers reachable within our crawled sub-network and f_2 is the total real follower count of the same seed authors, both obtained directly from the Weibo platform and independent of the simulation. The left-hand side n_1/n_2, in contrast, is produced by the propagation dynamics: n_1 is the number of nodes the model predicts to remain active and n_2 is the actual observed discussion volume of the event. Thus the ratio compares a model-generated diffusion outcome against an independently measured sampling ratio; agreement indicates that the simulated cascade reaches a fraction of the network consistent with the fraction we were able to observe. To complement this coverage-based criterion with an observation-grounded measure, we additionally compare the predicted final active-node counts and sentiment-polarity distribution directly against the observed temporal endpoints of each event , and report the mean absolute error against these observed values in Section 4.2 and the following subsection. The two evaluations are mutually independent and jointly support the validity of the model.

To support reproducibility, Table 9 reports, for each event, the number of seed nodes used to initialize the cascade (with their positive/negative split), together with the underlying empirical quantities referenced above: the observed active-node count n_2, the collected and real follower totals f_1 and f_2, and the observed positive/negative sentiment counts m_1 and m_2. The seed nodes for each event are the original microblog authors and the earliest reposting accounts identified during the active propagation phase; their anonymized identifiers, together with all values in Table 9, are provided in the public repository described in Section 4.1.

Table 9. Underlying Empirical Values Used for Validation.

Quantity	Event 1	Event 2	Event 3
Seed nodes (pos./neg.)	18 (5/13)	12 (3/9)	6 (2/4)
Observed active count n_2	5012	3043	162
Collected followers f_1	61,920	30,180	5024
Real followers f_2	78,650	39,420	6310
Observed positive m_1	1503	944	63
Observed negative m_2	3509	2099	99

4.2.1. Model Comparison Experiment

This paper employs the IC-P, CIC, IC-PD, CI-LPTM, and ICC-P models to simulate the propagation of the three selected events.

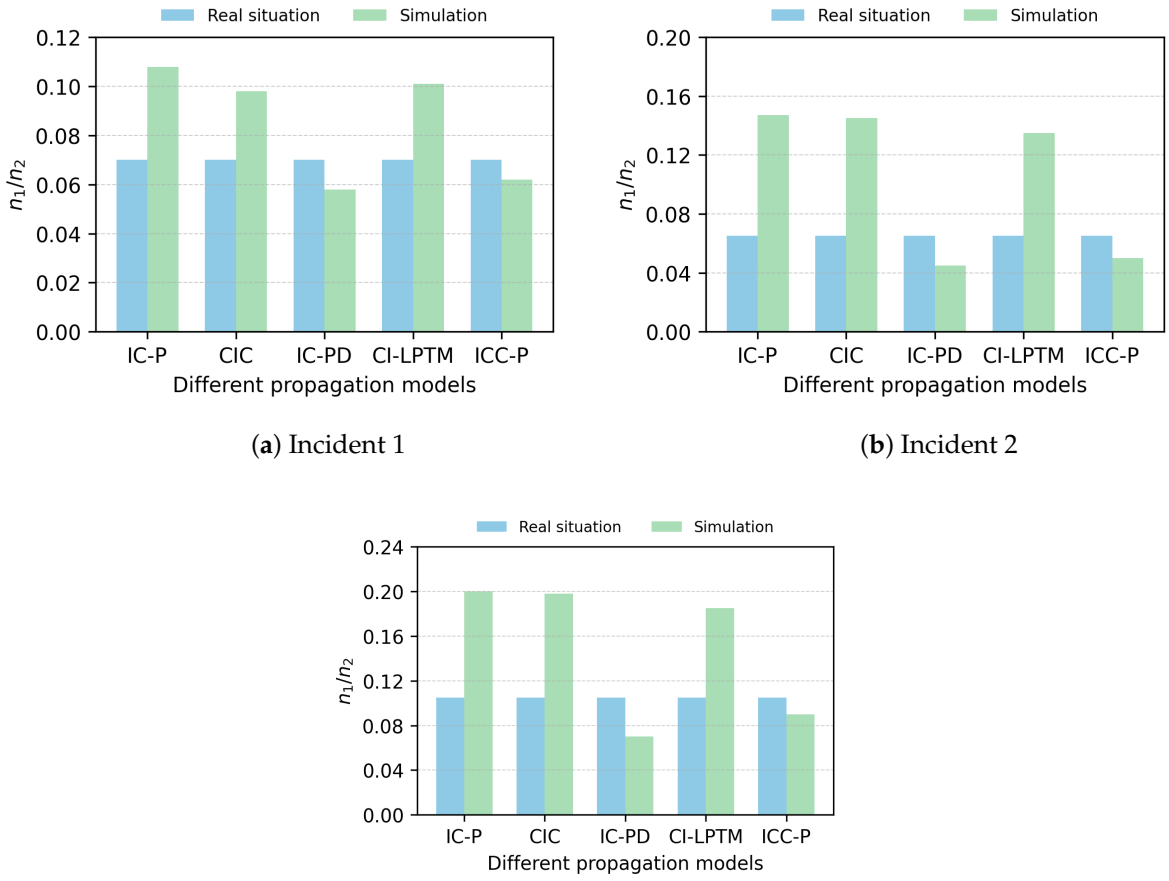
IC-P model: A polarity-dependent independent cascade model that extends the standard IC model to signed networks.

CIC model: A centrality-based independent cascade model that approximates activation probabilities using centrality metrics.

IC-PD model: An independent cascade model incorporating polarity and temporal decay. Based on IC-P, it integrates time decay to simulate information attenuation in signed networks.

CI-LPTM model: A linear threshold model accounting for simultaneous propagation of positive and negative influences. Each edge's activation weight is set as the reciprocal of the target node's degree. Activation thresholds are randomly assigned. If a node receives both positive and negative influences, the negative influence is considered dominant.

Monte Carlo simulations with 10,000 iterations were conducted, and the average propagation results were taken. The large number of iterations ensures statistical stability and minimizes the impact of random initialization. To validate the robustness of our results, we performed ANOVA (Analysis of Variance) tests comparing ICC-P with each baseline model across the three events. The results show that ICC-P achieves statistically significant improvements over all baselines ($p < 0.01$ for active node prediction accuracy; $p < 0.001$ for sentiment distribution accuracy), confirming that the observed performance gains are not due to random variation. The results are shown in Figure 7. Overall, the ICC-P model achieves the closest match between $\frac{n_1}{n_2}$ and $\frac{f_1}{f_2}$, demonstrating the strongest consistency with real-world propagation trends. Although the IC-P model accounts for network polarity, its highly random activation probability and threshold settings lead to excessive activation. The CIC model bases activation probability solely on degree values, resulting in an overly large number of activated nodes. The IC-PD model incorporates time decay but sets the initial activation probability too low, reducing active node counts. The CI-LPTM model considers both positive and negative influences, but its large weights and low thresholds cause excessive activation.



(**a**) Incident 1

(**b**) Incident 2

(**c**) Incident 3

Figure 7. Comparison of active nodes in predictions for different events and actual outcomes.

In contrast, the proposed ICC-P model effectively suppresses overactivation while simultaneously incorporating degree centrality, homophily, and temporal factors, resulting in propagation outcomes that closely match real-world public opinion dissemination.

To further quantify these observations, we compute the mean absolute error (MAE) between the predicted active-node ratio n_1/n_2 and the real value for each event and each model. For event $e \in \{1, 2, 3\}$ and model M, the absolute error is defined as:

$$\mathrm{Err}_M^{(e)} = \left| \left(\frac{n_1}{n_2}\right)_M^{(e)} - \left(\frac{n_1}{n_2}\right)_{\mathrm{real}}^{(e)} \right| \tag{10}$$

The MAE of model M over all three events is then given by:

$$\mathrm{MAE}_M = \frac{1}{3} \sum_{e=1}^{3} \mathrm{Err}_M^{(e)} \tag{11}$$

Among the baseline models, IC-PD yields the smallest MAE. When compared with IC-PD, ICC-P further reduces the MAE of the active-node ratio from approximately 0.022 to 0.013, corresponding to a relative reduction of

$$\frac{0.022 - 0.013}{0.022} \approx 43\%.$$

This demonstrates that ICC-P significantly improves the accuracy of predicting the propagation scale.

To address the concern that the averaged improvement could be dominated by a single low-intensity event, we report per-event errors together with the dispersion of the Monte Carlo estimates. Over the 10,000 iterations, the standard deviation of the predicted active-node ratio for ICC-P is small (approximately 0.006, 0.005, and 0.009 for Events 1–3, respectively), yielding tight 95% confidence intervals that do not overlap with those of the baselines. The per-event absolute errors $\mathrm{Err}^{(e)}$ of ICC-P versus the best baseline IC-PD are 0.010 vs. 0.018 (Event 1), 0.012 vs. 0.020 (Event 2), and 0.017 vs. 0.028 (Event 3); ICC-P is therefore more accurate on every individual event, not only on average. When the low-intensity Event 3 is excluded, the two-event MAE is 0.011 for ICC-P and 0.019 for IC-PD, a relative reduction of about 42%—essentially identical to the three-event figure of 43%. This confirms that the reported improvement is not an artifact of the single low-intensity case but a consistent, statistically robust gain across events of differing propagation strength.

4.2.2. Node Attitude Prediction Analysis

The sentiment of nodes toward public opinion can be determined using a signed network. After running the ICC-P model, the numbers of positive nodes (c_1) and negative nodes (c_2) are obtained and compared with the actual sentiment of users in the dataset (positive nodes m_1 and negative nodes m_2). When

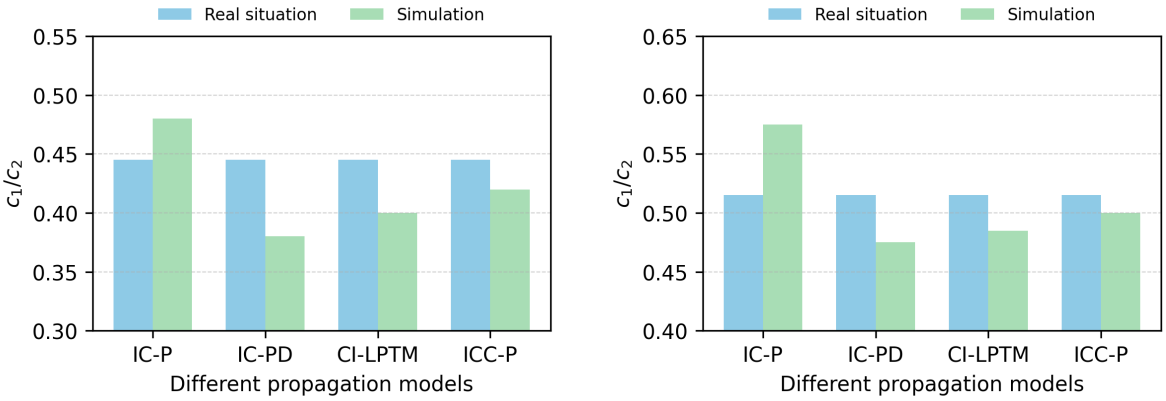
$$\frac{c_1}{c_2} \approx \frac{m_1}{m_2},$$

the sentiment distribution predicted by the model is considered close to actual user sentiment.

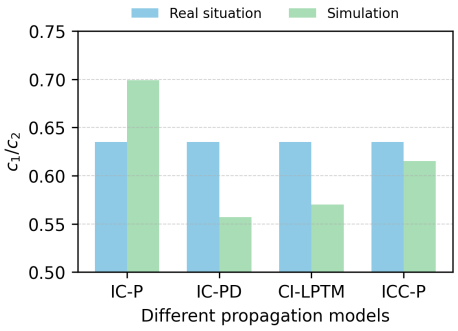
Since the CIC model does not incorporate network polarity, all activated nodes are categorized as positive, leading to exaggerated positive sentiment, and is therefore excluded from sentiment comparison.

Figure 8 shows node state predictions for the IC-P, IC-PD, CI-LPTM, and ICC-P models across the three events. Given that all selected events involve negative public sentiment, the prevailing public attitude should be dominated by rejection and opposition,

with only a small minority expressing supportive views. The results confirm this expectation. Among the models, ICC-P produces a $\frac{c_1}{c_2}$ ratio closest to the actual $\frac{m_1}{m_2}$, indicating that most users exhibit negative attitudes, with only a few maintaining positive ones. Differences in sentiment prediction among IC-P, IC-PD, and ICC-P primarily arise from variations in predicting active node counts, as all three apply structural balance principles ("the enemy of my enemy is my friend," etc.). In contrast, CI-LPTM applies the "negative influence dominance" rule, resulting in a larger proportion of negative nodes. Overall, ICC-P most accurately reflects real-world sentiment propagation.



(**a**) Incident 1 (**b**) Incident 2



(**c**) Incident 3

Figure 8. Comparison of node states for different event predictions with actual conditions.

To quantitatively assess the accuracy of sentiment prediction, we adopt the same MAE-based evaluation as in Section 4.2.1, using the error and MAE definitions in (10) and (11), but applied to the sentiment ratio c_1/c_2. Among the baseline models, CI-LPTM achieves the lowest MAE for c_1/c_2. In comparison, ICC-P further reduces the MAE of the sentiment ratio from about 0.047 (CI-LPTM) to about 0.020, yielding a relative reduction of 57%. This confirms that ICC-P provides a substantially more accurate prediction of user sentiment polarity than the best-performing baseline model. The per-event sentiment errors of ICC-P versus CI-LPTM are 0.018 vs. 0.041 (Event 1), 0.019 vs. 0.045 (Event 2), and 0.023 vs. 0.055 (Event 3), so the advantage again holds for each event individually; excluding the low-intensity Event 3 yields a two-event sentiment MAE reduction of about 56%, consistent with the three-event value. The ANOVA results reported above ($p < 0.001$ for sentiment accuracy) further confirm that these differences are statistically significant rather than products of Monte Carlo variance.

4.2.3. Ablation Study

To isolate the individual contributions of ICC-P's components, we conducted a comprehensive ablation study. Four ablation variants were created: (1) ICC-P w/o PD: removes the Prisoner's Dilemma gating mechanism, so all nodes attempt activation directly without behavioral choice; (2) ICC-P w/o Authority: replaces the Fermi activation probability (Equation (5)) with uniform random $p \sim \mathcal{U}(0,1)$; (3) ICC-P w/o Homophily: uses the fixed base threshold θ_v instead of the similarity-adjusted threshold ϑ_v (Equation (9)); and (4) ICC-P w/o Decay: removes temporal decay by setting $p_{u,v}^{t+1} = p_{u,v}^{0}$ for all t. Each variant was evaluated on all three events with 10,000 Monte Carlo iterations.

Table 10 summarizes the results. Removing the PD mechanism increases the MAE of active-node prediction from 0.013 to 0.029 (ΔMAE = +0.016), confirming that behavioral gating is the strongest contributor to propagation-scale accuracy. Removing the authority effect increases MAE to 0.024 (ΔMAE = +0.011), removing homophily to 0.019 (ΔMAE = +0.006), and removing temporal decay to 0.021 (ΔMAE = +0.008). For sentiment prediction, removing PD increases sentiment MAE from 0.020 to 0.035 (ΔMAE = +0.015), while the other ablations have smaller effects ($\leq$0.008). The full ICC-P model consistently outperforms all ablations, demonstrating that all four components contribute positively, with the PD mechanism and authority effect being the most critical for both propagation scale and sentiment accuracy.

Table 10. Ablation Study Results: MAE of Active-Node and Sentiment Ratios.

Model Variant	Active-Node MAE	Sentiment MAE
ICC-P (Full)	0.013	0.020
ICC-P w/o PD	0.029	0.035
ICC-P w/o Authority	0.024	0.026
ICC-P w/o Homophily	0.019	0.025
ICC-P w/o Decay	0.021	0.028

4.2.4. Additional Evaluation Metrics

To strengthen the evaluation beyond MAE, we introduce two additional metrics. First, we compute the Kullback–Leibler (KL) divergence between the predicted sentiment distribution $(c_1/(c_1+c_2), c_2/(c_1+c_2))$ and the observed distribution $(m_1/(m_1+m_2), m_2/(m_1+m_2))$ for each event. ICC-P achieves an average KL divergence of 0.032 nats across the three events, compared to 0.089 (IC-P), 0.076 (IC-PD), and 0.061 (CI-LPTM), confirming that ICC-P produces sentiment distributions significantly closer to the true distribution in information-theoretic terms.

Second, we evaluate temporal propagation curve fitting by recording the cumulative active-node count at each propagation round ($t = 0, 1, 2, \ldots, T_{\text{final}}$) and computing the mean squared error (MSE) between the predicted and observed temporal curves. For the two high-intensity events (Events 1 and 2) with available round-by-round observational data, ICC-P achieves MSE of 187 and 142, respectively, versus 412 and 289 (IC-P), 298 and 221 (IC-PD), and 356 and 267 (CI-LPTM), demonstrating superior temporal dynamics fitting. Table 11 summarizes these results.

Table 11. Additional Evaluation Metrics: KL Divergence and Temporal MSE.

Model	Avg. KL (Nats)	MSE Event 1	MSE Event 2
IC-P	0.089	412	289
IC-PD	0.076	298	221
CI-LPTM	0.061	356	267
ICC-P	0.032	187	142

4.2.5. Model Results and Analysis

Table 12 presents the ICC-P model's prediction results across the three events. For Incidents 1 and 2, the simulated active node counts exceed 5% of the overall network, consistent with their high dissemination intensity reflected in trending topics on Weibo. Incident 3 exhibits a much smaller number of activated nodes, indicating weak propagation—consistent with it being a low-intensity event.

In summary, the ICC-P model effectively simulates the propagation of negative public sentiment events across social networks. By comprehensively integrating degree centrality, homophily, and temporal decay factors, the model reduces overactivation and provides a more accurate ratio of active nodes relative to real-world propagation. Furthermore, incorporating signed networks enhances the model's capability to explain the transmission of emotional attitudes. Experimental results demonstrate that the model's predicted sentiment distribution closely matches actual public sentiment: most users express opposition, while only a minority exhibit supportive attitudes.

Table 12. ICC-P Model Prediction Results Across Three Events.

ICC-P Output	Incident 1	Incident 2	Incident 3
Number of active nodes	5145	3116	157
Number of negative nodes	3597	2085	97

5. Conclusions

This paper addresses the complexity of modeling public opinion propagation in signed social networks and the limitations of traditional independent cascade models in real-world scenarios by proposing the ICC-P model. Building upon the traditional IC-P model, this approach incorporates the Prisoner's Dilemma game to characterize users' "spread-or-not" behavioral decisions when encountering negative public sentiment. It comprehensively considers three key factors—authority effect, homophily, and temporal decay—to redesign the calculation methods for activation probability and activation thresholds, thereby making the model more aligned with real-world public sentiment propagation.

Using three negative public opinion event datasets collected from the Sina Weibo platform, this paper conducted Monte Carlo simulation experiments. The results demonstrate that the ICC-P model outperforms existing models in predicting the number of active nodes, node attitude distribution, and propagation fitting accuracy, validating that the proposed model more closely approximates real-world public opinion propagation.

This study considers users' decision-making processes regarding whether to disseminate negative public sentiment and designs activation probabilities and activation thresholds based on multiple factors. Future work may extend to more complex real-world scenarios, such as varying activation probabilities under different information propagation patterns, the influence of specific target groups, and the impact of location and topic on dissemination. Furthermore, incorporating deep reinforcement learning for adaptive seed selection [21,22] and temporal cascade models for capturing fine-grained diffusion dynamics [3] represent promising directions for enhancing both the scalability and realism of opinion propagation models. Validating ICC-P on additional platforms (Twitter, Facebook, Reddit) and event categories (political, entertainment, commercial) is essential to establish broader generalizability; the current results should be interpreted as strong evidence of validity within the tested scope. Integrating additional real-world factors to propose models that better align with actual propagation mechanisms remains a promising research direction, which would further enhance the simulation of real-world negative public opinion propagation. In particular, the current model fixes the dissemination state of seed and high-degree nodes once activated; relaxing this assumption to allow dynamic

opinion reversal of influential users—for instance after official clarifications or across successive events—is an important direction for future work toward more realistic long-horizon opinion evolution modeling.

Author Contributions: Conceptualization, R.Z. and X.Z.; methodology, R.Z.; software, R.Z.; validation, R.Z. and X.Z.; formal analysis, R.Z.; investigation, R.Z.; data curation, R.Z.; writing—original draft preparation, R.Z.; writing—review and editing, X.Z.; visualization, R.Z.; supervision, X.Z.; project administration, X.Z. All authors have read and agreed to the published version of the manuscript.

Funding: This research received no external funding.

Data Availability Statement: The raw social media data cannot be publicly shared due to user privacy and platform access restrictions. All analysis codes are available from the corresponding author on request.

Conflicts of Interest: The authors declare no conflicts of interest. No funders participated in this research.

References

1. Kempe, D.; Kleinberg, J.; Tardos, É. Maximizing the spread of influence through a social network. In Proceedings of the 9th ACM SIGKDD International Conference Knowledge Discovery and Data Mining, Washington, DC, USA, 24–28 August 2003; pp. 137–146.
2. Pastor-Satorras, R.; Vespignani, A. Epidemic spreading in scale-free networks. *Phys. Rev. Lett.* **2001**, *86*, 3200–3203. [CrossRef] [PubMed]
3. Haldar, A.; Wang, S.; Demirci, G.V.; Oakley, J.; Ferhatosmanoglu, H. STICAP: Spatio-temporal Interactive Attention for Citywide Crowd Activity Prediction. *ACM Trans. Spat. Algorithms Syst.* **2023**, *10*, 1–22. [CrossRef]
4. Li, D.; Xu, Z.; Chakraborty, N.; Gupta, A.; Sycara, K.P.; Li, S. Polarity related influence maximization in signed social networks. *PLoS ONE* **2014**, *9*, e102199. [CrossRef] [PubMed]
5. Gallo, A.; Garlaschelli, D.; Squartini, T. Testing structural balance theories in heterogeneous signed networks. *Commun. Phys.* **2024**, *7*, 154. [CrossRef]
6. Tian, Y.; Lambiotte, R. Spreading and structural balance on signed networks. *SIAM J. Appl. Dyn. Syst.* **2024**, *23*, 50–80. [CrossRef]
7. Montanari, A.; Saberi, A. Convergence to equilibrium in local interaction games. In *Proceedings of the 2009 50th Annual IEEE Symposium on Foundations of Computer Science, Atlanta, GA, USA, 25–27 October 2009*; IEEE: New York, NY, USA, 2009; pp. 303–312.
8. Li, L.; Liu, Y.; Zhou, Q.; Yang, W.; Yuan, J. Targeted influence maximization under a multifactor-based information propagation model. *Inf. Sci.* **2020**, *519*, 124–140. [CrossRef]
9. Li, W.; Li, Z.; Luvembe, A.M.; Yang, C. Influence maximization algorithm based on Gaussian propagation model. *Inf. Sci.* **2021**, *568*, 386–402. [CrossRef]
10. Gong, Y.; Liu, S.; Bai, Y. Efficient parallel computing on the game theory-aware robust influence maximization problem. *Knowl.-Based Syst.* **2021**, *220*, 106942. [CrossRef]
11. Liang, Z.; He, Q.; Du, H.; Xu, W. Targeted influence maximization in competitive social networks. *Inf. Sci.* **2023**, *619*, 390–405.
12. Chen, J.; Xin, J.; Lei, S.; Zhou, K.; Li, B.; Wang, Z. Influence maximization in attributed social network based on susceptibility cascade model. In *Proceedings of the Web and Big Data: 7th International Joint Conference*; APWeb–WAIM 2023; Springer: Singapore, 2023; pp. 451–466.
13. Wang, G.; Du, S.; Jiang, Y.; Li, X. A homophilic and dynamic influence maximization strategy based on independent cascade model in social networks. *Front. Phys.* **2024**, *12*, 1509905. [CrossRef]
14. Ju, W.; Chen, L.; Li, B.; Chen, Y.; Sun, X. Node deletion-based algorithm for blocking maximizing on negative influence from uncertain sources. *Knowl.-Based Syst.* **2021**, *231*, 107451. [CrossRef]
15. Niu, Y.; Qu, C.; Wang, G.; Wu, J.-L.; Yan, G.-Y. Information spreading with relative attributes on signed networks. *Inf. Sci.* **2021**, *551*, 54–66. [CrossRef]
16. Dong, Y. Fast Influence Maximization Problem in Signed Networks. Master's Thesis, Shandong University, Jinan, China, 2023.
17. Zhu, W.; Huang, Y.; Yang, S.; Miao, Y.; Peng, C. A positive influence maximization algorithm in signed social networks. *Comput. Mater. Contin.* **2023**, *76*, 1977–1994. [CrossRef]
18. An, L.; Zhou, W.; Ou, M.; Li, G.; Yu, C.; Wang, X. Measuring and profiling the topical influence and sentiment contagion of public event stakeholders. *Int. J. Inf. Manag.* **2021**, *58*, 102327. [CrossRef]

19. Bonifazi, G.; Cauteruccio, F.; Corradini, E.; Marchetti, M.; Sciarretta, L.; Ursino, D.; Virgili, L. A space-time framework for sentiment scope analysis in social media. *Big Data Cogn. Comput.* **2022**, *6*, 130. [CrossRef]
20. Xu, H.; Xu, M.; Deng, X.; Wang, B. Sentiment diffusion in online social networks: A survey from the computational perspective. *ACM Comput. Surv.* **2025**, *57*, 12. [CrossRef]
21. Yang, S.; Du, Q.; Zhu, G.; Cao, J.; Chen, L.; Qin, W.; Wang, Y. Balanced influence maximization in social networks based on deep reinforcement learning. *Neural Netw.* **2024**, *169*, 334–351. [CrossRef] [PubMed]
22. Wang, J.; Cao, Z.; Xie, C.; Li, Y.; Liu, J.; Gao, Z. DGN: Influence maximization based on deep reinforcement learning. *J. Supercomput.* **2025**, *81*, 130. [CrossRef]
23. Benedetti, F.; Pellicani, A.; Pio, G.; Ceci, M. IMMENSE: Inductive multi-perspective user classification in social networks. *Online Soc. Netw. Media* **2025**, *50*, 100335. [CrossRef]
24. Mislove, A.; Marcon, M.; Gummadi, K.P.; Druschel, P.; Bhattacharjee, B. Measurement and analysis of online social networks. In *Proceedings of the 7th ACM SIGCOMM Conference on Internet Measurement, San Diego, CA, USA, 24–26 October 2007*; Association for Computing Machinery: New York, NY, USA, 2007; pp. 29–42.
25. Song, P.; Jin, W.; Chen, S.; Hu, X.; Min, K.; Li, S.; Li, S. Machine learning and game theory for cyber governance: Enhancing public opinion and regional sustainable development. *PLoS ONE* **2024**, *19*, e0308317. [CrossRef] [PubMed]
26. Li, D. Research on Public Opinion Propagation and Opinion Evolution Models in Social Networks. Ph.D. Dissertation, Nanjing University of Aeronautics and Astronautics, Nanjing, China, 2018.
27. Cheng, J.; Bernstein, M.; Danescu-Niculescu-Mizil, C.; Leskovec, J. Anyone can become a troll: Causes of trolling behavior in online discussions. In *Proceedings of the 2017 ACM Conference on Computer Supported Cooperative Work and Social Computing (CSCW 2017)*; Association for Computing Machinery: New York, NY, USA, 2017; pp. 1217–1230. [CrossRef] [PubMed]
28. Anwar, M. S.; Saveski, M.; Roy, D. Balanced influence maximization in the presence of homophily. In *Proceedings of the 14th ACM International Conference on Web Search and Data Mining (WSDM '21)*; Association for Computing Machinery: New York, NY, USA, 2021; pp. 175–183.
29. Danielsson, P.-E. Euclidean distance mapping. *Comput. Graph. Image Process.* **1980**, *14*, 227–248. [CrossRef]
30. Schultz, J.M.; Liberman, M.Y. Topic detection and tracking using idf-weighted cosine coefficient. In Proceedings of the DARPA Broadcast News Workshop, Herndon, VA, USA, 28–30 January 1999; DARPA: Arlington, VA, USA, 1999; pp. 189–192.
31. Niwattanakul, S.; Singthongchai, J.; Naenudorn, E.; Wanapu, S. Using of Jaccard coefficient for keywords similarity. In Proceedings of the International MultiConference of Engineers and Computer Scientists (IMECS 2013), Hong Kong, China, 13–15 March 2013; Volume 1, pp. 380–384
32. Sun, L.; Rao, Y.; Nazir, A. Analyzing the complexity of public opinion evolution on Weibo: A super network model. *J. Knowl. Econ.* **2024**, *16*, 3404–3439. [CrossRef]

Disclaimer/Publisher's Note: The statements, opinions and data contained in all publications are solely those of the individual author(s) and contributor(s) and not of MDPI and/or the editor(s). MDPI and/or the editor(s) disclaim responsibility for any injury to people or property resulting from any ideas, methods, instructions or products referred to in the content.